

Selective Reduction of NO_x with Propene under Oxidative Conditions: Nature of the Active Sites on Copper-Based Catalysts

C. Márquez-Alvarez,[†] I. Rodríguez-Ramos,[†] A. Guerrero-Ruiz,[‡] G. L. Haller,^{*,§} and M. Fernández-García^{†,§}

Contribution from the Instituto de Catálisis y Petroleoquímica, CSIC, Campus Cantoblanco, 28049-Madrid, Spain, Departamento Química Inorgánica, UNED, Senda del Rey, 28040-Madrid, Spain, and Department of Chemical Engineering, Yale University, 9 Hillhouse Avenue, New Haven, Connecticut 06520-8286

Received May 15, 1996[⊗]

Abstract: The chemical changes that occurred in two copper-based catalysts (Cu-ZSM-5 and Cu-Al₂O₃) during the selective reduction of NO with propene in the presence of oxygen were studied using *in situ* X-ray absorption near edge structure (XANES). For the quantitative analysis of the XANES spectra, a mathematical procedure based on evolving factor analysis (EFA) has been applied. Correlation with catalytic data shows that copper is fully oxidized in both systems when the conversion of propene is complete and the conversion of NO to N₂ reaches its maximum value. The XANES analysis together with comparison of the catalytic behavior of Cu-ZSM-5 with Cu-Al₂O₃ and Cu-SiO₂ systems indicates that the rate limiting step of the reaction takes place on cupric oxides (although other species may also participate). This conclusion is of general significance because it establishes the physical basis for the role of Cu in selective catalytic reduction of NO by hydrocarbons; this explains the recently recognized fact that zeolitic supports do not play an essential role in the reaction and that the mechanism may not involve a Cu²⁺/Cu¹⁺ redox cycle or, if it does, the cycle is dominated by the oxidized species. *In situ* XANES analysis coupled with EFA is demonstrated to be a useful technique to obtain information about the active sites present on a catalyst during reaction.

Introduction

Selective catalytic reduction of nitrogen oxides with hydrocarbons (SCR-HC) is receiving much attention due to the ever-growing number of diesel-powered vehicles. Conversion of the pollutant NO_x into nitrogen cannot be achieved by traditional three-way catalysts (TWC) under the net oxidizing conditions that exist in the exhaust gases of diesel and other lean-burn engines.¹ Base metal oxides supported on alumina, cation-exchanged zeolites, and acidic solids have been explored as alternatives to present noble metal catalysts.² Among these systems, Cu-exchanged ZSM-5 zeolite is one of the most studied since the early work of Iwamoto³ showed the high turnover rates exhibited by this catalyst for nitric oxide decomposition.

Despite the extensive existing literature, the mechanism of SCR-HC catalyzed by Cu-ZSM-5 has not yet been fully clarified.⁴ Besides the (apparent) contradictory conclusions developed concerning the role that zeolite acid sites play in the overall reaction mechanism, the effects of the excess oxygen are not well established. It has been shown that reaction does not take place without oxygen, but this has been attributed to different causes. One is the possible formation of NO₂ as a key intermediate. The partial oxidation of hydrocarbon mol-

ecules to generate H_xC_yO_z species that could be the active reductant for NO_x has been suggested also. Finally, oxygen could play an essential role by maintaining the copper atoms in an appropriate oxidation state. Likewise, both Cu²⁺⁵ and Cu⁺⁶ have been proposed as the active center.

The Cu role in the SCR-HC reaction is also a matter of controversy. While EPR experiments show that copper is fully oxidized at temperatures at which maximum activity is observed,^{7,8} the XANES study of Liu and Robota⁹ suggests, by using a normalized difference edge method, i.e., changes in the absorbance at 8983 eV are considered to be produced by a Cu(II)/Cu(I) redox process, that the catalytic activity is related to the evolution of Cu(I), concluding that these reduced centers are the active sites. In addition to the uncertainty of the oxidation state, there is no clear indication of the nature of the active sites; this comes from the fact that several copper chemical species can co-exist inside the zeolite channels. The first type corresponds, obviously, to exchanged species. EPR studies¹¹ detected two Cu²⁺ signals and ascribed them to 5- and 4-coordinated copper species, with square-pyramidal and square-planar geometries, respectively. These EPR studies are complemented by theoretical calculations which allow prediction of the local geometries of Cu²⁺/Cu⁺ ions or [Cu(OH)]⁺ com-

* To whom correspondence should be addressed.

[†] CSIC.

[‡] UNED.

[§] Yale University.

[⊗] Abstract published in *Advance ACS Abstracts*, February 15, 1997.

(1) Taylor, K. C. In *Catalysis: Science and Technology*; Anderson, J. R., Boudart, M., Eds.; Springer-Verlag: New York, 1984; Vol. 5, p 120.

(2) Kapteijn, F.; Stegenga, S.; Dekker, N. J. J.; Bijsterbosch, J. W.; Moulijn, J. A. *Catal. Today* **1993**, *16*, 273.

(3) Iwamoto, M.; Furukawa, H.; Mine, Y.; Uemura, G.; Mikuriya, S.; Kagawa, S. *J. Chem. Soc., Chem. Commun.* **1986**, 1272.

(4) Shelef, M. *Chem. Rev.* **1995**, *95*, 209 and references therein.

(5) d'Itri, J. L.; Sachtler, W. M. H. *Catal. Lett.* **1992**, *15*, 289.

(6) Burch, R.; Millington, P. J. *Appl. Catal. B: Environ.* **1993**, *2*, 101.

(7) Petunchi, J. O.; Hall, W. K. *Appl. Catal. B: Environ.* **1993**, *2*, L17.

(8) Kucherov, A. V.; Gerlock, J. L.; Jen, H.-W.; Shelef, M. *Catal. Today* **1996**, *27*, 79.

(9) (a) Liu, D. J.; Robota, H. J. *Appl. Catal. B: Environ.* **1994**, *4*, 155.

(b) Kharas, K. C. C.; Liu, D. J.; Robota, H. J. *Catal. Today* **1995**, *26*, 129.

(10) (a) Kau, L.-S.; Spira-Solomon, J.; Penner-Hahn, J. E.; Hodgson, K. O.; Solomon, E. I. *J. Am. Chem. Soc.* **1987**, *109*, 6433. (b) Smith, T. A.; Penner-Han, J. E.; Hodgson, K. O.; Barding, M. A.; Doniach, S. *EXAFS and Near Edge Structure III*; Proc. Int. Conf.; Hodgson, K. O., Hedman, B., Penner-Han, J. E., Eds.; Spriger-Verlag: New York, 1984.

plexes.¹² Cu^{2+} ions compensating charge of 2 Al^{3+} ions for 6 and 5 unit rings shows 2-fold and 5-fold coordinations,^{12c} possibly the latter being characteristic of "square-pyramidal" geometries, i.e., geometries with ligands in the three spatial directions. Hass and Schneider^{12b} found a stable nearly square-planar coordination (ligands accumulated close to a plane containing the central Cu^{2+} ion) for copper cations located in a two Al-substituted 6-membered ring. The $[\text{Cu}(\text{OH})]^+$ complex^{12c} and Cu^+ ion¹² are both predicted to have 2-fold coordination, although there is not general agreement about the local symmetry of the last species, claimed to be nonlinear by the more sophisticated calculations^{12b,c} and linear by ref 12a. The second type corresponds to oxo complexes that have been proposed as Cu dimers $[\text{Cu}^{2+}-\text{O}^{2-}-\text{Cu}^{2+}]$ on the basis of UV-vis, IR, and TPR studies.¹³ However, ZSM-5 Cu-oxo complexes are EPR silent species, in contrast to other Cu pair complexes observed in Y-zeolite or oxides such as ceria.¹⁴ This point suggests either that this type of species contains a small, although undetermined, number of Cu and O ions (in the 2:1 ratio established by TPR) or that this strong interaction induces a large difference in the conformation of the Cu pair with respect to Y-zeolite or ceria systems. In this case, the Cu^{2+} ions complete their coordination spheres with both lattice and extralattice oxygen anions. On reduction, the link between Cu^{2+} ions disappears or weakens notably, yielding "isolated" Cu^+ cations.^{13,15} The third type of chemical species corresponds to small copper oxide particles located in the zeolite cavities.¹⁵ The three types of species show different behavior when interacting with reactants such as H_2 , CO , and NO ¹⁵ as well as differences in the $\text{Cu}^{2+}-\text{O}^{2-}$ bond characteristics,^{13,15} showing that Cu ions must have very different environments in each one of these species. Given that Cu exchanged ions are mostly coordinated to lattice oxygen, oxidic Cu ions coordinated to extralattice oxygen, and Cu ions inserted in oxo complexes to both kinds of oxygen, the last statement is by no means a surprise.

A XANES study may shed some light on the understanding of both the oxidation state and chemical environment of Cu under reaction conditions. Therefore, with the goal to establish the nature of the catalytically active sites of copper-based catalysts during the selective catalytic reduction of NO with propene, here we report a detailed chemical description of the copper species present during reaction. The catalysts are studied by XANES during reaction and spectra are analyzed by a statistical method to determine the number of copper species. Using this method, a full chemical description of the active phases can be achieved. Site-selective XANES may also be used to selectively probe different chemical species in a sample. Site-selective XANES has been previously accomplished with ion-desorption detection, luminescence or fluorescence detection, X-ray standing waves, and diffraction anomalous fine structure (DAFS) [see ref 16 for further details]. However, for catalytic

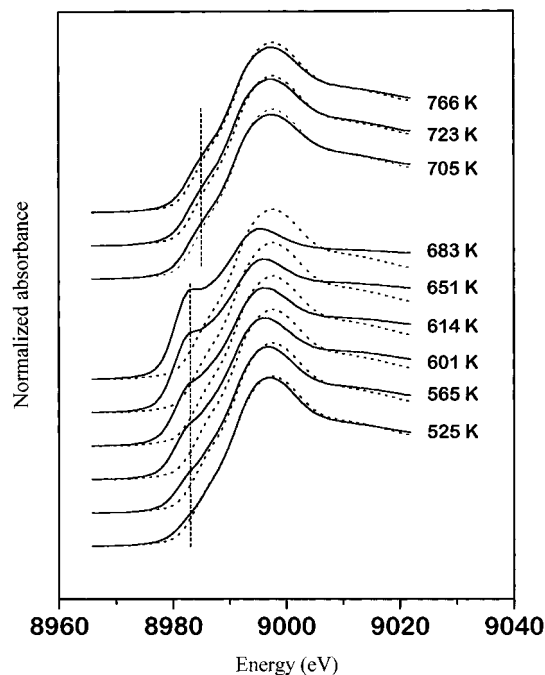


Figure 1. Cu K-edge XANES spectra of Cu-ZSM-5 catalyst under $\text{NO} + \text{C}_3\text{H}_6 + \text{O}_2/\text{He}$ at increasing temperatures (full lines). The spectrum of the pre-oxidized sample is shown as a broken line. Dashed lines drawn indicate 8983- and 8985-eV energies.

samples, i.e., samples with only short range order studied at atmospheric pressures, site-selective detection is only possible using luminescence or fluorescence that yields spectra with very low signal-to-noise ratio and, of course, with minor interferences of co-existent species.¹⁶ Therefore, accurate determination of a species contribution to a spectrum is usually impossible to obtain with site-selective XANES and the statistical analysis of absorption XANES data appears to be the only alternative to carefully follow the solid-state phase under reaction conditions. The statistical analysis used here will generate XANES spectra for all copper chemical species present during reaction and will determine their concentration as a function of the reaction temperature. Evolution of these species is correlated with catalytic activity. The study of this correlation, performed in two Cu-based catalysts (Cu-ZSM-5 and $\text{Cu}-\text{Al}_2\text{O}_3$), will show that selective catalytic reduction of NO by hydrocarbons can be performed in any Cu-based system containing small cupric oxide particles and some acidity at reaction temperatures.

Results and Discussion

(A) Copper Chemical State. Figure 1 shows selected XANES spectra of the Cu-ZSM-5 catalyst under the $\text{NO} + \text{C}_3\text{H}_6$

(11) (a) Kucherov, A. V.; Slinkin, A. A.; Kondrat ev, D. A.; Bondarenko, T. N.; Rubinstein, A. M.; Minachev, Kh. M. *Kinet. Catal.* **1985**, *26*, 353; *Zeolites* **1985**, *5*, 320. (b) Grünert, W.; Hayes, N. W.; Joyner, R. W.; Shpiro, E. S.; Siddiqui, M. R. H.; Baeva, G. *J. Phys. Chem.* **1994**, *98*, 10832. (c) Dedecek, J.; Sobalík, Z.; Tvaruzková, Z.; Kaucky, D.; Wichterlová, B. *J. Phys. Chem.* **1995**, *99*, 16327.

(12) (a) Sayle, D. C.; Perrin, M. A.; Nortier, P.; Catlow, C. R. A. *J. Chem. Soc., Chem. Commun.* **1995**, 945. (b) Hass, K. C.; Schneider, W. F. *J. Phys. Chem.* In press. (c) Trout, B. L.; Chakraborty, A. K.; Bell, A. T. *J. Phys. Chem.* **1996**, *100*, 4173.

(13) Lei, G.-D.; Adelman, B. J.; Sárkány, J.; Sachtler, W. M. H. *Appl. Catal. B: Environ.* **1995**, *5*, 245.

(14) (a) Clao, C. C.; Lunsford, J. H. *J. Chem. Phys.* **1972**, *57*, 2890. (b) Aboukais, A.; Bennani, A.; Aissi, C. F.; Wrobel, G.; Guelton, M.; Vedrine, J. *J. Chem. Soc., Faraday Trans.* **1992**, *88*, 615.

(15) Beutel, T.; Sárkány, J.; Lei, G.-D.; Yan, J. Y.; Sachtler, W. M. H. *J. Phys. Chem.* **1996**, *100*, 845.

(16) Grush, M. M.; Christou, G.; Hamalainen, K.; Cramer, S. P. *J. Am. Chem. Soc.* **1995**, *117*, 5895.

(17) Costa, E.; Uguina, M. A.; de Lucas, A.; Blanes, J. *J. Catal.* **1987**, *107*, 317.

(18) Sepúlveda-Escribano, A.; Márquez, C.; Rodríguez-Ramos, I.; Guerrero-Ruiz, A.; Fierro, J. L. G. *Surf. Interf. Anal.* **1993**, *20*, 1067.

(19) Guerrero-Ruiz, A.; Rodríguez-Ramos, I.; Fierro, J. L. G. *Appl. Catal.* **1991**, *72*, 119.

(20) de Boor, C. *A Practical Guide to Splines*; Springer-Verlag: New York, 1978.

(21) Malinowski, E. R. *Factor Analysis in Chemistry*, 2nd ed.; Wiley: New York, 1991.

(22) Press, W. H.; Teukolsky, S. A.; Vetterling, W. T.; Flannery, B. P. *Numerical Recipes in Fortran*, 2nd ed.; Cambridge Press: Cambridge, 1992.

(23) Fernández-García, M.; Márquez-Alvarez, C.; Haller, G. L. *J. Phys. Chem.* **1995**, *99*, 12565.

(24) Malinowski, E. R. *J. Chemom.* **1990**, *4*, 102.

(25) Fiedor, J. N.; Proctor, A.; Howalla, M.; Hercules, D. M. *Surf. Interface Anal.* **1993**, *20*, 1.

Table 1. Principal Components Analysis Results

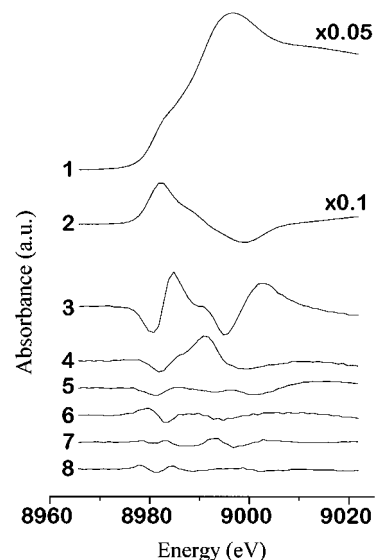
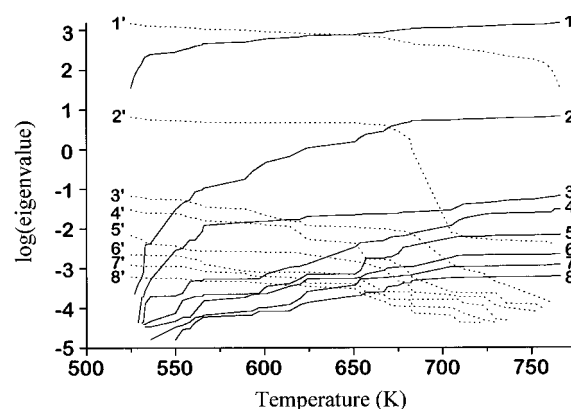
component	eigenvalue	% SL	REVR	variance ^a
1	827.24	0.00	208.6	99.537
2	3.7940	0.00	101.4	0.457
3	0.035729	0.04	3.1	0.004
4	0.011028	0.14	3.3	0.001
5	0.003143	1.48	2.1	
6	0.001402	3.53	2.0	
7	0.000664	7.96	1.7	
8	0.000378	12.65	1.7	
9	0.000208	21.04	1.2	

^a Variance is given in percentage. Values lower than 10^{-3} are not reported.

+ O_2/He mixture at increasing temperatures. Broken lines correspond to the sample under pure oxygen, after pre-treatment at 773 K. Comparison of the spectra during reaction with that of the oxidized sample evidences evolution of a shoulder at ca. 8983 eV, already present at the beginning of the reaction, and which increases with temperature up to 683 K. Such a feature, characteristic of the $1s \rightarrow 4p$ transition in 2- and 3-coordinated Cu(I) complexes,¹⁰ shows that Cu(II) species are reduced under the reaction mixture and progressive reduction is observed up to 683 K. Above 700 K, the feature at 8983 eV disappears and spectra become close to that of the oxidized sample. No shape changes are observed at increasing temperatures from 705 to 773 K. Between 683 and 705 K, the sample is completely re-oxidized and remains unaltered at higher temperatures. The general trend observed agrees well with that reported by Liu and Robota⁹ for an *over-exchanged* Cu-ZSM-5 catalyst under similar conditions. However, we found a relationship between catalytic activity and concentration of Cu(II) and Cu(I) species opposite to that obtained by Liu and Robota (see below). XANES spectra of Cu-ZSM-5 re-oxidized during reaction (spectra at $T \geq 705$ K in Figure 1) show slight differences in the edge shape (around 8985 eV) compared with the pre-treated sample. This clearly indicates the presence of a second Cu(II) species, whose edge shape is characteristic of a D_{4h} coordination.¹⁰ Thus, at least two Cu(II) species can be identified. One or two Cu(I) species may be generated, depending on whether these two Cu(II) species yield the same or a different Cu(I) compound on reduction. These results suggest, as expected, that there is a minimum of three, probably four, species that can be identified in the whole set of spectra.

After calcination, the active metal in Cu- Al_2O_3 is inserted in CuO-like and superficial CuAl₂O₄ matrices in nearly equal quantities.²⁶ XANES spectra of the Cu- Al_2O_3 sample during reaction show the presence of these Cu(II) species only and no changes are observed with increasing reaction temperature. For the sake of brevity and because the initial spectrum remains unaltered, a figure with these spectra is omitted.

(B) Factor Analysis. Identification of Copper Species. In order to determine the number of copper species and quantify their concentrations in Cu-ZSM-5 along the reaction, the set of XANES spectra has been submitted to FA. Calculated eigenvalues together with their respective variance, reduced eigenvalues ratio (REVR), and the percentage of significance level (%SL) for the F-test are shown in Table 1. Assuming a 5% test level for the % SL, the F-test would indicate a number of

**Figure 2.** Abstract spectral components (R_{abs} matrix).**Figure 3.** Evolving factor analysis diagram: forward (full lines) and backward (broken lines).

principal factors (pure species) of 6. However, in this case, the biggest increase in the % SL value does not correspond to such a test level, in contrast with previous results.^{23,26} The % SL for component number five is ten times larger than that of the fourth component, while the sixth and seventh components only double the value of their prior values. This evolution in % SL may suggest that the number of factors may be only 4. Therefore, it seems that the F-test does not provide a definite answer. In addition, REVR values only indicate a large difference in the significance degree of the first two components, with a continuous decrease in REVR values from the third and higher components.

Analysis of the abstract row matrix (spectral components), with the first eight columns represented in Figure 2, indicates that components number one, two, and three are mainly signal. Component four seems to have also some signal contribution, while components five and six apparently contain mainly low-frequency background errors.

The previous analysis suggests that there are four copper species that can be identified in the whole set of XANES spectra, although it is not clear if the number could be extended up to six. To establish beyond doubt if the 5th and 6th components contain only *noise*, we use evolving factor analysis (EFA). The results for forward (full lines) and backward (broken lines) EFA are shown in Figure 3. Eigenvalues have been sorted in a decreasing order for every temperature, and only the eight largest eigenvalues are presented (named 1, 2, ..., 8 for forward and 1', 2', ..., 8' for backward EFA). To obtain the number of

(26) Fernández-García, M.; Márquez-Alvarez, C.; Rodríguez-Ramos, I.; Guerrero-Ruiz, A.; Haller, G. L. *J. Phys. Chem.* **1995**, *99*, 16380.

(27) Gemperline, P. J.; Hamilton, J. C. In *Computer-Enhanced Analytical Spectroscopy*; Meuzelar, L. C., Ed.; Plenum: New York, 1990; Vol. 2, p 40.

(28) Maeder, M. *Anal. Chem.* **1987**, *59*, 527.

(29) Gemperline, P. J. *J. Chem. Inf. Comput. Sci.* **1984**, *24*, 206.

(30) Harman, H. H. *Modern Factor Analysis*, 3rd ed.; The University of Chicago Press: Chicago, 1976.

species and determine the corresponding temperatures at which they appear and disappear, it is necessary first to deduce the *noise* level in the EFA diagram. This level outlines the pool of error eigenvalues above which a given eigenvalue is determined to represent a chemical species. In this case, the *noise* level can be obtained from backward EFA curves. As may be seen in Figure 1, spectra at temperatures between 705 and 773 K are essentially identical to each other. Thus, the signal in this temperature range may be represented by a single spectrum, whatever the number of spectra taken. In other words, factor analysis of a **D** matrix containing only spectra in this region will identify a single primary eigenvector. It has been indicated before that these spectra correspond to, at least, two Cu(II) species. However, from the point of view of the mathematical description, there is no information that allows one to identify more than one species when looking only at the spectra corresponding to $T \geq 705$ K. Therefore, in the backward EFA, from 773 to 705 K, only eigenvalue 1' can correspond to signal, while the rest are noise. This permits us to determine the *noise level* from eigenvalue 2' and to fix it at about 3×10^{-3} . Then, an eigenvalue emerging from this level will indicate that a new species is appearing. The chemical description from Figure 1 is now used to assign every eigenvalue to a certain copper species (reduced or oxidized), according to the temperature range in which they exist. As disappearance of a given species in forward EFA generally corresponds to appearance in backward EFA, such ranges are better defined by taking together both curves for every species.

In the forward EFA, there are four eigenvalues emerging from the pool of noise. Curve 1 increases continuously from 523 to 773 K, indicating that the related species exists over the whole temperature range. Therefore, this eigenvalue should be assigned to an oxidized species ($\text{Cu}^{\text{II}}_{\text{A}}$). Eigenvalue 2 is also larger than the noise level from approximately the beginning of the reaction and increases with temperature up to ca. 675 K. The other two species appear at higher temperatures, namely ca. 560 K for species number three and 675 K for species number four. Therefore, at temperatures below 560 K only two copper species are identified. As the coexistence of Cu(II) and Cu(I) species has been established at these temperatures, eigenvalue 2 must be related to a reduced center ($\text{Cu}^{\text{I}}_{\text{B}}$). Its absence above 700 K agrees with the re-oxidation process already described. The temperatures at which eigenvalues 3 and 4 emerge from the pool of noise suggest that they correspond to reduced ($\text{Cu}^{\text{I}}_{\text{A}}$) and oxidized ($\text{Cu}^{\text{II}}_{\text{B}}$) species, respectively. This is supported by analysis of the backward EFA curves.

Four eigenvalues exceed the noise level ($\log[\text{eigenvalue}] \sim -2.5$) in the backward EFA. As indicated above, in the region 773–705 K, only one principal component is observed, although it is truly a combination of, at least, two Cu(II) species. This is more clearly seen when adding the next column (spectrum at 683 K) to the **D** matrix containing spectra from 773 to 705 K. As shown in Figure 3, addition of this new column produces a sharp increase in eigenvalue 2' as well as the rise of eigenvalue 3' just above the pool of noise, with little effect on eigenvalue 1'. That is, three species are identified at 683 K. Two of them are Cu(II) species already present at 773–705 K and, according to the spectrum shape (Figure 1, spectrum at 683 K), the third one must be a Cu(I) species. The smallest eigenvalue (3') is ascribed to the reduced species, and the largest (1' and 2') to oxidized ones. This is based on the fact that only a single column in this reduced data matrix (temperature range: 683–773 K) contains a Cu(I) contribution, while the remaining present contributions of Cu(II) species only. The appearance of the eigenvalue 2' with a large increase is explained as due to

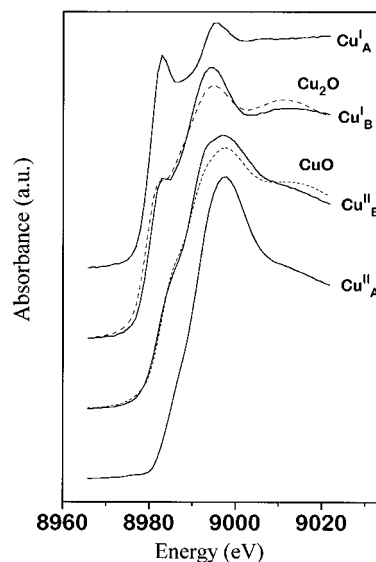


Figure 4. XANES spectra of pure copper species (full lines) obtained by FA of the Cu-ZSM-5 spectra set. Spectra of bulk copper oxides (broken lines) are also shown for comparison.

change in the set of eigenvectors. From 773 to 705 K, only one signal eigenvector is obtained, representing a constant combination of two species. The addition of the column corresponding to 683 K, besides generating a new eigenvalue associated with a Cu(I) species, introduces the necessary information to allow discrimination between the two Cu(II) species. As a consequence, the previous eigenvector (1') is split into two new vectors (1' and 2'). The last backward eigenvalue, 4', appears well below 683 K.

In conclusion, EFA results show that only four species, two Cu(II) and two Cu(I), are present during the experiment. One of the oxidic species, $\text{Cu}^{\text{II}}_{\text{A}}$, exists at all temperatures (eigenvalues 1–1') while the second, $\text{Cu}^{\text{II}}_{\text{B}}$, only appears around 683 K, being observed at higher temperatures. This last species is connected with eigenvalues 4–2' although its existence cannot be inferred in the usual way of interpreting EFA results; the discussion given in previous paragraphs indicates that its region of existence is defined by eigenvalue 4. Because the reduced species have a limited temperature region of existence, the forward and backward eigenvalues associated with them should cross. Therefore, one of the Cu(I), $\text{Cu}^{\text{I}}_{\text{B}}$, exists from the starting temperature up to about 625 K (eigenvalues 2–4') and the second Cu(I) is observed from about 560 to 683 K (eigenvalues 3–3'). No other crossing is likely to occur as eigenvalues 3 and 4' cross just above the noise level, defining a narrow window of existence which does not have any visible consequence in Figure 1. As will be shown in the forthcoming discussion, these regions compare fairly well with the ones extracted from ITFA.

Once the number of factors has been established, the abstract **R** and **C** matrices are obtained. Their adequate rotation by the ITFA procedure gives the final solution, which is represented in Figure 4 (**R**_{real} matrix) and Figure 5 (**C**_{real} matrix). Figure 4 shows the four spectral components defined by FA (full lines). XANES spectra of Cu(I) and Cu(II) oxides registered with the same experimental equipment are shown (broken lines) as references. A tentative identification of copper phases can be drawn from Figure 4. Spectra of $\text{Cu}^{\text{I}}_{\text{A}}$ and $\text{Cu}^{\text{I}}_{\text{B}}$ exhibit a pre-edge feature at 8983 eV characteristic of transition $1s \rightarrow 4p$ in Cu(I) complexes.¹⁰ For this reason, these spectra are attributed to reduced (Cu^{I}) species. Spectra $\text{Cu}^{\text{II}}_{\text{A}}$ and $\text{Cu}^{\text{II}}_{\text{B}}$ are then assigned to the oxidized species, in agreement with their edge shape. Given the high sensitivity of the XANES spectrum shape

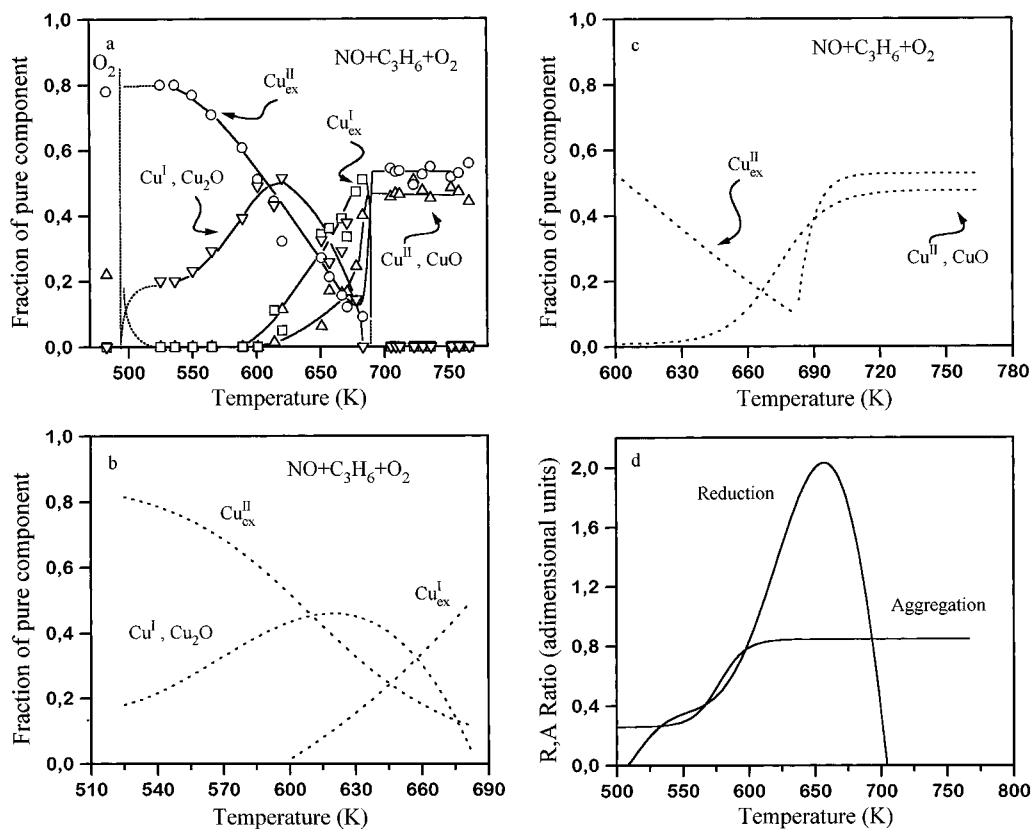


Figure 5. (a) Relative concentration of pure species in Cu-ZSM-5 during reaction under $\text{NO} + \text{C}_3\text{H}_6 + \text{O}_2/\text{He}$. Symbols to the left of the dotted line correspond to pre-oxidized sample. (○) $\text{Cu}^{\text{II}}_{\text{ex}}$; (△) $\text{Cu}^{\text{II}}, \text{CuO}$; (□) $\text{Cu}^{\text{I}}_{\text{ex}}$; (▽), $\text{Cu}^{\text{I}}, \text{Cu}_2\text{O}$. (b) Low-temperature trends of the concentration profiles. (c) High-temperature trends of the concentration profiles. (d) Aggregation and reduction/oxidation behavior of the sample (see text for details).

to coordination distances (as continuum resonances depend on the coordination distance as r^{-2}) and local symmetry, the shape similarity between $\text{Cu}^{\text{II}}_{\text{B}}$ and CuO spectra strongly suggests that $\text{Cu}^{\text{II}}_{\text{B}}$ species correspond to a cupric oxide (-like) phase.

This assignment is consistent with results reported by Beutel et al.,¹⁵ who identified copper oxide particles on Cu-ZSM-5 samples at ion exchange levels over 40%. Due to the small size of ZSM-5 zeolite channels (ca. 5.1–5.7 Å), this phase ($\text{Cu}^{\text{II}}_{\text{B}}$) would correspond to small CuO aggregates. This limited particle size and/or a strong interaction with zeolite walls, or with the chemisorbed layer, could explain the small differences observed in the intensity of the continuum resonances (not in their positions nor in the shape of the edge region) between the $\text{Cu}^{\text{II}}_{\text{B}}$ spectrum and the spectrum of a well-crystallized bulk CuO . Besides, this assignment is more likely than Cu^{2+} ions in 5- or, particularly, in 4-coordinated exchange positions of ZSM-5 because the predicted minimum energy Cu^{2+} species¹² have symmetries lower than D_{4h} that do not have the XANES shape (characteristic shoulder at about 8985 eV) observed in Figures 1 and 4, and/or $\text{Cu}^{2+}-\text{O}$ distances clearly different than those in CuO . Also, the local symmetry and coordination distances expected from the XANES spectrum shape of $\text{Cu}^{\text{II}}_{\text{B}}$ species make possible the elimination of a $[\text{Cu}(\text{OH})]^+$ assignment.^{12c} The oxo-complex option can be disregarded also because, as noted in the introduction, this species should have different (Cu) local geometry than the one corresponding to cupric oxide. Additionally, it can be mentioned that appearance of oxo complexes is usually favored by performing the exchange at higher pH and calcining at higher temperature than the ones used here.¹⁵ In short, it seems that the geometrical constraints of the zeolite cavities produce oxidized copper (exchanged or oxo complexes) species with a local environment quite different from that of a cupric matrix. Following this line of argument,

$\text{Cu}^{\text{I}}_{\text{B}}$ can be attributed to small Cu_2O particles inside the zeolite channels. Although it has been proposed that Cu^+ ions exchanged in the zeolite matrix have a 2-fold coordination, like Cu_2O , all the calculated coordinations¹² indicate that both phases may be easily differentiated through their XANES spectra. Sayle et al.^{12a} calculate $\text{Cu}^{\text{I}}-\text{O}$ distances in exchanged species around 2.4 Å while in cuprite it is observed with a single distance of 1.85 Å.³¹ Hass and Schneider^{12b} and Trout et al.^{12c} predict Cu^+-O distances below 2.0 Å, but with a nonlinear geometry. In this case, the $1s \rightarrow 4p_{xy}$ (where z is the Cu^+-O bond direction, see ref 10) transition will be strongly perturbed with respect to the one corresponding to linear geometry (Cu_2O) because the $4p_{xy}$ degeneracy will be destroyed. Therefore, the close energy positions of the pre-edge features and continuum resonances showed in Figure 4 by $\text{Cu}^{\text{I}}_{\text{B}}$ and bulk Cu_2O strongly suggest the assignment mentioned above. The $\text{Cu}^{\text{II}}_{\text{A}}$ spectrum shape agrees well with that of a flattened or distorted tetragonal $\text{Cu}(\text{II})$ complex with lower symmetry than T_d/D_{4h} (D_{2h} , C_{4v} , D_{2d} , S_4 , ...),¹⁰ as expected for Cu^{2+} isolated ions in exchange positions in the zeolite cavities. Finally, $\text{Cu}^{\text{I}}_{\text{A}}$ could be reasonably ascribed to Cu^+ -exchanged ions in ZSM-5. Its strong $1s \rightarrow 4p$ intensity is typical of two-coordinated $\text{Cu}(\text{I})$ complexes (Cu_2O excluded),¹⁰ in accordance with the predicted geometry for Cu^+ ions in ZSM-5.¹²

Therefore, two oxidized and two reduced, two aggregated and two exchanged species are detected in the sample. It is worth mentioning here that Liu and Robota⁹ observed a small positive energy shift in the $1s \rightarrow 4p$ transition peak of Cu^{I} species throughout the temperature region of existence of reduced species and suggested that two Cu^{I} species were evolving when increasing the temperature. They proposed that

both species could correspond to Cu^+ exchanged ions coordinated with two oxygen atoms. The analysis outlined above has also identified and quantified two Cu^{I} species behaving in a similar way to that reported in ref 9. However, it has been shown that the spectrum shape of the species appearing at lower temperature suggests a Cu_2O -like species rather than a Cu^+ exchanged ion.

An additional point deserving comment is whether or not the spectra of Figure 4 reveal some sign of interaction between the solid species and the reactants. We have already mentioned that the aggregated phases might be electronically perturbed by the presence of adsorbates. Liu and Robota⁹ suggest a more drastic effect, proposing that the shape of the $\text{Cu}^{\text{I}}_{\text{A}}$ (Cu^+_{ex}) species may be affected by propene (probably forming a π -allylic intermediate). Obviously, a pronounced effect of the reactant molecules may not be ascribed to this Cu^{I} species and may exert some influence in the other $\text{Cu}^{\text{I}}/\text{Cu}^{\text{II}}$ line shape XANES spectra. Note, however, that this possible influence is not decisive in the CuO - and Cu_2O -like species as evidences the comparison with bulk reference spectra; the similar edge shape and close proximity of continuum resonances allow one to unequivocally state the chemical nature of the ligands, their distance to the Cu central ion, and local symmetry. Thus, the differences in the intensity of the continuum resonances limit the possible effect of reactants to an electronic interaction typical of chemisorption. The lack of reference spectra prevents a similar observation being made for the exchanged species.

The relative concentration of the four copper species at every temperature (the final solution for the C_{real} matrix) is presented in Figure 5a. The values for the oxidized sample before contact with the reaction mixture are also shown (left side of dashed line). Figures 5b and 5c give details of the low- and high-temperature behavior, respectively, of the sample that will be discussed below. In Figure 5d the aggregation and reduction phenomena occurring during the temperature-programmed reaction are presented. The aggregation curve corresponds to the smoothed ratio between the fractional concentration profiles of aggregated species (CuO -like + Cu_2O -like) and exchanged ones, while the reduction state of the sample is represented by the smoothed ratio of the reduced species (Cu_2O -like + Cu^+_{ex}), fractional concentration, and oxidized species (CuO -like + $\text{Cu}^{2+}_{\text{ex}}$).

The results obtained using Factor Analysis (Figures 4 and 5) agree well with the coordination of copper species found in Cu-ZSM-5 by Cu^+ photoluminescence, EPR, and theoretical calculations.^{11,12} However, we found only a single Cu^{2+} -exchanged species instead of the two (4- and 5-fold) coordination environments generally proposed in the literature. Maybe our "low" exchange level induces the predominance of one species. An alternative reason for this may be the similarity between both symmetries, as the distorted square-planar coordination may be indistinguishable by XANES from the C_{4v} symmetry of the square-pyramidal coordination. Also, oxo complexes are not observed, probably due to their limited presence (below our detection limit) induced by the exchange conditions used. On the other hand, it is important to stress again that the present results clearly show that $\text{CuO}/\text{Cu}_2\text{O}$ -like species can be readily differentiated from $\text{Cu}^{2+}/\text{Cu}^+$ exchanged ions or oxo complexes using this statistical procedure because of the different local symmetries and/or coordination distances exhibited for these two groups of species.

(C) Chemical and Catalytic Issues. Assuming the previous assignment made for copper species, the concentration profiles shown in Figure 5 provide a description of the chemical evolution of the Cu-ZSM-5 sample with temperature in the

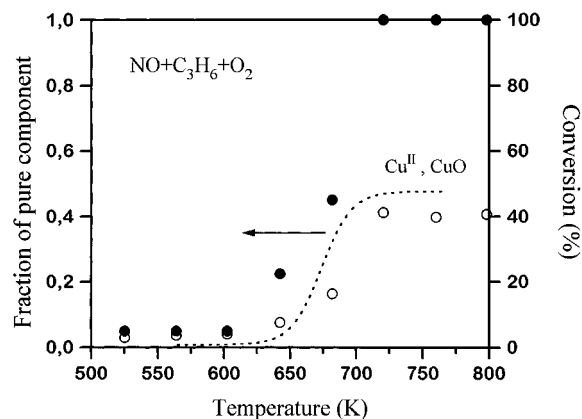


Figure 6. Catalytic activity for reduction of NO to N_2 (○) and oxidation of C_3H_6 to CO_2 (●), and concentration profile of CuO (dotted line).

reaction mixture. The chemical evolution of the sample is compared with its catalytic activity in Figure 6. Symbols in this later figure represent the normalized activities for reduction of NO to N_2 (open symbols) and total oxidation of propene (filled symbols), corresponding to a maximum conversion of 42% to N_2 and 100% to CO_2 . The dotted line is the concentration profile of CuO taken from Figure 5. We found a good relationship between the oxidized Cu(II) species concentration and the activity of the catalyst. This result is completely different from that reported by Liu and Robota,⁹ but note that both the $\text{NO}/\text{C}_3\text{H}_6$ ratio and the absolute concentration they used were lower. However, as outlined above, our XANES spectra (Figure 1) show a trend similar to that reported by Liu and Robota. Moreover, if one compares the concentration of the different copper species (Figure 5) and the NO conversion data used by Liu and Robota, taken from a previous paper of Iwamoto et al.,³² one can arrive at the same conclusion, "the variation of Cu(I) concentration with temperature seems to correlate well with NO conversion data". The concern is that the catalytic behavior of the Cu-ZSM-5 system is affected by variables such as the catalyst preparation method, the copper exchange degree, the acidity of the zeolite, etc. Therefore, in order to establish a conclusive correlation the chemical evolution of the catalyst should be compared with the catalytic activity and selectivity of the same catalyst.

The Cu-ZSM-5 sample pretreated under oxygen (Figure 5) has approximately 80% of the copper atoms as Cu^{2+} ions in zeolite exchange positions and 20% in a CuO -like phase. The initial existence of a CuO -like phase is a direct consequence of the preparation conditions (pH and Cu content); the existence of this phase on samples prepared similarly has been reported already.¹⁵ In the $\text{NO} + \text{C}_3\text{H}_6 + \text{O}_2/\text{He}$ mixture at 523 K, even though the reaction mixture is net oxidizing, the cupric oxide phase is reduced to cuprous oxide. This fact indicates that at low temperature the adsorption of propene is favored with respect to O_2 or NO_x . Previously, the adsorption of hydrocarbons has been observed to quickly reach equilibrium on bulk copper oxide during catalytic oxidation of hydrocarbons with oxygen.³³ As the temperature increases, an increase in the Cu_2O fraction in the Cu-ZSM-5 sample is observed. Simultaneously, the population of Cu^{2+} -exchanged species diminishes by an equivalent amount (Figure 5b). This evolution can therefore be interpreted as due to migration of Cu^{2+} ions, which aggregate in oxide particles that are easily reduced to Cu_2O . The segregation of the less reducible Cu^{2+} -exchanged ions can also

(32) Iwamoto, M.; Mizuno, N.; Yahiro, H. *Sekiyu Gakkaishi* **1991**, *34*, 375.

(33) Moro-oka, Y.; Morikawa, Y.; Ozaki, A. *J. Catal.* **1967**, *7*, 23.

be related to the adsorption of propene on these ions. Likewise, in Cu-exchanged Y-zeolite adsorption of propene has been shown to produce migration of copper ions.³⁴ Figure 5b indicates that the mobility of copper ions increases with temperature, in agreement with previous results on Cu-Y.³⁴ Note that the NO molecule may also act as a reductant and this is particularly so with the high NO concentrations we have used (24 000), although the above discussion as well as that made by Kharas et al.^{9b} for previous published XANES results clearly give the principal role of this competition to the hydrocarbon. However, it is conceivable that NO could be involved in the reduction of copper species containing very weakly bonded oxygen, i.e. oxo complexes. Nevertheless, it has been shown in section B above that a significant amount of the oxo-complex species is absent in our sample and thus limits the influence of this possible process in the present case.

At 590 K, a temperature at which both reactions, the reduction of nitric oxide and the oxidation of propene, start (Figure 6), an increase in Cu⁺-exchanged species following the decrease in Cu²⁺-exchanged species is observed (Figure 5b). At a slightly higher temperature, ca. 620 K, the concentration of the Cu₂O phase begins to fall and that of CuO is augmented by an equivalent amount. Such evolution in the concentration of the four species in the range 590–683 K suggests that isolated Cu²⁺ ions are reduced to Cu⁺ while Cu₂O particles are oxidized to CuO without further extension of the Cu migration process. Re-oxidation of this Cu₂O-like phase is complete at 683 K. Parallel to these processes an increase in the activity is observed (Figure 6). Around 705 K (Figures 5c,d), Cu⁺ ions are suddenly re-oxidized to Cu²⁺. The overall reduction/oxidation process (Figure 5d) has a temperature dependence, i.e., an S-shape at low temperatures and a strong decay above 700 K, quite similar to those reported in refs 8 and 9. Above 700 K the conversion of propene is total (Figure 6) and that of the NO reaches its maximum level (42%), and both are stable up to the end of the experiment. In this temperature range, the catalyst is fully oxidized but a larger concentration in CuO-like phase is observed with respect to the sample before reaction. This increment in the CuO-like/Cu²⁺-exchanged ratio (calculated on an atomic Cu basis) is in agreement with the already mentioned increased intensity observed, with respect to the spectrum before reaction, at 8985 eV in the XANES spectra taken at 700–773 K. It is important to stress that this behavior is not unique to our sample, the same phenomenon can be observed when carefully comparing the spectra reported by Liu and Robota (Figure 2 in ref 9; note that a value of 8985 eV in the energy scale of Figure 1 corresponds to 6–7 eV on Liu and Robota's scale).

In sum, we can see that for Cu-ZSM-5 samples with a (theoretical) level of exchange close to or higher than 100%, all the studies reported in the literature^{8,9} are consistent with the existence of two phenomena, aggregation and reduction, during temperature-programmed reaction. This work reveals that both are adsorbate-induced effects produced by the higher energy of adsorption of propene with respect to other reactants. In spite of the fact that these phenomena have no effect on the reaction kinetics (occur at low temperatures, at which no NO or C₃H₆ conversion is observed) they certainly influence the catalytic behavior of the sample by changing the Cu phase distribution. A secondary conclusion of this analysis is that the aggregated phase has an easier redox Cu(II)/Cu(I) conversion than the exchanged one; this may reflect some steric effect on the redox processes taking place on the second type of centers.

(34) Coudurier, G.; Decamp, T.; Praliaud, H. *J. Chem. Soc., Faraday Trans. 1* **1982**, 78, 2661.

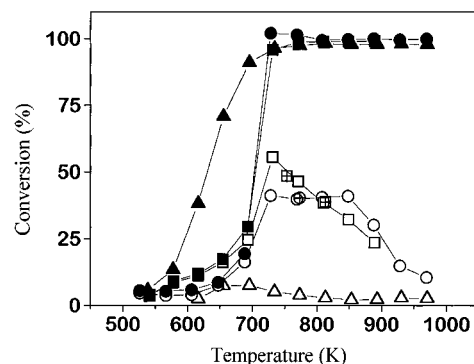


Figure 7. Catalytic activity for reduction of NO to N₂ (open symbols) and for oxidation of C₃H₆ to CO₂ (solid symbols) over (Δ, ▲) Cu-SiO₂, (□, ■) Cu-Al₂O₃, and (○, ●) Cu-ZSM-5 at increasing temperature. Circles and boxes with a cross indicate N₂ conversion obtained while cooling.

At higher temperatures, where reaction occurs, the oxidized state of Cu suggests that Cu(II) centers (either exchanged and/or CuO-like species) catalyze the selective reduction of NO with propene. This conclusion agrees with the EPR results of Kucherov et al.⁸ and Petunchi et al.³⁵ The oxidized state of Cu is also consistent with the rate limiting step proposed by Cowan et al.;³⁶ these authors showed that the abstraction of hydrogen from the hydrocarbon is the rate limiting step, and subsequent work suggests that this process is assisted by oxidized-NO (NO₂-type) species adsorbed on Cu(II) sites.³⁷ Note that an assisted H-abstraction rate limiting step is also consistent with a non-redox mechanism or, at least, with the fact that a redox pathway does not need to be invoked as a key step. However, Figure 6 provides additional information not presented in the literature; it shows a strong correlation between the CuO-like phase and the NO conversion; when CuO is not present no catalytic activity is observed and, after its appearance, it seems that activity follows closely the increase of CuO amount up to about 705 K, when complete burning of the hydrocarbon is reached.

To further support the XANES results, in particular, the last conclusion in the previous paragraph, the catalytic behavior of the Cu-ZSM-5 and Cu-Al₂O₃ samples is shown in Figure 7. The XANES spectra of this latter catalyst, under reaction conditions, also exhibit the presence of Cu(II) species only. In Figure 7, open symbols represent the conversion of NO into N₂ and solid symbols the corresponding conversion of C₃H₆ into CO₂, measured at a constant heating rate. The performance of both catalysts is quite similar, showing nearly the same light-off temperature for propene oxidation and nitric oxide reduction (ca. 700 K). N₂ yield increases until full hydrocarbon oxidation is obtained and falls at high temperatures. This deactivation is known to be reversible and high N₂ conversion values are produced when cooling the catalyst (see Figure 7, crossed symbols). In our experimental conditions, the Cu-Al₂O₃ sample shows a higher activity toward nitric oxide reduction than Cu-ZSM-5 does. However, it has to be taken into account that this activity is not referred per exposed active site. Besides, as can be observed from the extensive literature,⁴ light-off tem-

(35) Petunchi, J. O.; Sill, G.; Hall, W. K. *Appl. Catal. B: Environ.* **1993**, 2, 303.

(36) Cowan, A. D.; Dumpelmann, R.; Cant, N. W. *J. Catal.* **1995**, 151, 356.

(37) Adelman, B. J.; Beutel, T.; Lei, G.-D.; Sachtler, W. M. H. *J. Catal.* **1996**, 158, 327.

(38) Bethke, K. A.; Kung, M. C.; Yang, B.; Shah, M.; Alt, D.; Li, C.; Kung, H. H. *Catal. Today* **1995**, 26, 169.

(39) Centi, G.; Perathoner, S.; Dall'Olio, L. *Appl. Catal. B: Environ.* **1994**, 4, L275.

(40) Shelef, M. *Catal. Lett.* **1994**, 26, 277.

perature, maximum activity, and the overall conversion-vs-temperature profile vary with copper content, catalyst preparation, and catalytic test conditions for a given support. Thus, a general comparison of Cu-Al₂O₃ vs Cu-ZSM-5 catalysts cannot be drawn from these results. On the other hand, this fact again shows that it is necessary that chemical characterization by XANES be compared with catalytic data obtained from the same sample under equivalent reaction conditions, as already stated.

The rather similar catalytic behavior of Cu-ZSM-5 and Cu-Al₂O₃ samples shown in Figure 7 again suggests that cupric oxide, the common phase in both samples, catalyzes the selective reduction of NO with propene and that zeolite exchanged copper species or oxo complexes do not play an exclusive role in the SCR-HR reaction mechanism. We must stress that our results concern highly loaded (80%) Cu-ZSM-5 systems, and for lower loadings, zeolite related species may play an important role. For samples with a theoretical level of exchange close to 100%, ref 37 shows that a nitrate-type species adsorbed on cupric oxide is the fastest intermediate that reacts with propene yielding N₂. However, propene reacts with several nitrogen-containing species which concentrations are dependent on the sample level of exchange, precluding an easy generalization of this result. On the other hand, a CuO-like active phase is indirectly supported by data reported by d'Itri and Sachtler,⁵ who observed a high activity for the selective reduction of NO with propene on a Cu-ZSM-5 sample prepared by impregnation, although solid state ion exchange may have occurred following impregnation. Also, a recent compilation of results reported by Bethke et al.³⁸ shows that SCR-HC is primarily affected by the nature of the active centers and not by the nature of the support. These authors mainly related catalytic activity with copper dispersion; however, the results reported by Centi et al.³⁹ on Cu-borolite clearly show that the activity for nitric oxide reduction is also influenced by the presence of Lewis acid sites. This is supported by the very low nitrogen conversion obtained with the impregnated Cu-SiO₂ samples (close to zero for 1 wt % Cu as for 15 wt % Cu; results for the Cu-SiO₂ sample with 15 wt % Cu content are shown in Figure 7) compared to catalysts with acidic supports like Cu-Al₂O₃ and Cu-ZSM-5, as already reported (see references in ref 38). This conclusion is apparently contradicted by the high activity reported for a 1 wt % Cu-SiO₂ sample prepared by gelation.³⁸ However, as this preparation method could lead to a certain Cu-Si compound and no indication of acidic properties of the sample is given, the essential role of acid sites cannot be ruled out.

It is well-known that acid centers catalyze the formation of carbonaceous deposits from propene (but not from propane) on Cu-ZSM-5,⁴⁰ but controversy exists on the exact role that these deposits might play in the SCR of NO.⁴ The IR results of Bell et al.⁴¹ as well as the known fact that dark-colored Cu-ZSM-5 samples (denoting the presence of carbonaceous residues originated by exposure to propene or to the reaction mixture at temperatures lower than 650 K) change to the original light blue once light-off is reached suggest that coke is not present in significant amounts at maximum conversion of NO. In any case, this coke does not seem to decisively influence the XANES spectrum of any Cu(II) species. This could be related to the fact that coke apparently occupies sites for which NO_x reduction intermediates do not compete.⁴¹ Finally, we point out the very low light-off temperature observed for the hydrocarbon oxidation reaction on Cu-SiO₂ compared to Cu-ZSM-5 and Cu-Al₂O₃ samples (Figure 7). As XANES results suggest that CuO particles in these two latter samples are very small, we can

interpret this result as due to the structure sensitivity of the hydrocarbon oxidation reaction.⁴²

Conclusions

Factor Analysis has been shown to provide an adequate method to interpret complex (multicomponent) XANES spectra and to obtain a quantitative distribution of the chemical species contributing to those spectra. A set of XANES spectra of an 80% exchanged Cu-ZSM-5 sample under a mixture of NO, C₃H₆, and excess O₂ diluted in He has been analyzed by this procedure. Two oxidized and two reduced copper species have been identified in the sample at temperatures between 523 and 773 K. These species have been ascribed to Cu²⁺ and Cu⁺ ions located in exchange positions inside the zeolite channels, and to small CuO and Cu₂O aggregates. The relative concentration of all four species changes with the reaction temperature. For comparison the XANES spectra of a Cu-Al₂O₃ sample under reaction have also been studied. The latter exhibits Cu(II) species (CuO-like and superficial CuAl₂O₄-like species) which are practically unaltered during the reaction ramp.

The study of the Cu-ZSM-5 sample by *in-situ* XANES spectroscopy, together with its interpretation by Factor Analysis, has provided a detailed chemical description of the copper species and their evolution during selective catalytic reduction of NO with propene. Adsorbate-induced reduction and segregation phenomena are observed at low temperatures in the presence of the reactive mixture. The correlation between copper species concentration profiles and catalytic activity supports a mechanism in which oxidized Cu(II) species are the centers where NO_x molecules are activated. Comparison with the Cu-Al₂O₃ sample indicates that copper in small oxide particles is catalytically active and that zeolite-exchanged Cu²⁺ ions and oxo complexes are not necessary for the selective reduction of NO.

Experimental and Computational Details

(A) Sample Preparation. Na-ZSM-5 parent zeolite, synthesized by a typical procedure¹⁷ using ethanol as a template, with Si/Al = 32 and Na/Al = 1.2 ratios (as determined by XRF analysis), was ion-exchanged in an aqueous solution of Cu(II) acetate (pH 6.5–7.0), washed with deionized water, dried at 383 K, and calcined in air at 673 K for 2 h. The final Cu-ZSM-5 catalyst was found to contain a 1.4 wt % Cu on a metal basis (measured by AA spectrometry), equivalent to 80% cationic exchange (assuming 2 Na⁺ cations are exchanged by one Cu²⁺).

For purposes of comparison, Cu-Al₂O₃ and Cu-SiO₂ catalysts were also studied. The Cu-Al₂O₃ sample was prepared by adsorption of copper from an aqueous solution of Cu(NO₃)₂·3H₂O (Merck reagent grade) on a γ -alumina (Puralox, Condea, S_{BET} = 200 m² g⁻¹) at pH 9. The Cu content of this sample is 1.6 wt %. Further details about this catalyst may be found elsewhere.¹⁸ The Cu-SiO₂ catalysts, with 1 and 15.1 wt % of Cu, were prepared by wet impregnation with a Cu(II) nitrate aqueous solution.¹⁹

Bulk copper oxides have been prepared as references for the analysis of Cu-ZSM-5 XANES spectra. CuO was obtained by calcining in air Cu(II) nitrate (Johnson-Matthey), at 673 K for 5 h, and Cu₂O by heating CuO powder (Merck) at 1073 K for 30 min under vacuum. X-ray diffractograms of both samples only showed peaks attributable to CuO (monocl) or Cu₂O (cub) phases, respectively.

(B) Catalytic Activity Measurements. The powdered Cu-ZSM-5, Cu-Al₂O₃, and Cu-SiO₂ samples were pressed, crushed, and sieved to 30–40 mesh, introduced into a U-shaped quartz microreactor (4 mm i.d.), held between quartz-wool pieces, and *in situ* pretreated in an oxygen flow at 773 K for 30 min. After the sample was cooled under oxygen to 523 K, the gas flow was changed to the reaction mixture (2.7% NO, 1.1% C₃H₆, and 10% O₂, balance helium, at atmospheric

(41) Bell, V. A.; Feeley, J. S.; Deeba, M.; Ferrauto, R. J. *Catal. Lett.* **1994**, *29*, 15.

(42) Márquez-Alvarez, C.; Guerrero-Ruiz, A.; Rodríguez-Ramos, I. Unpublished results.

pressure, GHSV = 36 000 h⁻¹), and the temperature was raised to 773 K at a constant heating rate of 1.25 K·min⁻¹. Gas mixtures were prepared with nitric oxide (3.00% in helium), propene (99.0%), and oxygen (99.98%), provided by SEO, without further purification. Flow rates were adjusted by using Brooks mass flow controllers. The composition of the reactor effluents was analyzed by a Varian 3400 gas chromatograph equipped with a TCD detector and Porapak Q and 5A molecular sieve columns.

(C) XANES Experiments. Transmission XANES measurements at the Cu K-edge were carried out at the Cornell High Energy Synchrotron Source (line CII), using a Si(111) double-crystal monochromator with 40% detuning to minimize the effects of higher harmonic frequencies. Samples were pressed into self-supported wafers with total absorbance 2 (bulk copper oxides were diluted in boron nitride). Reaction was followed in a controlled-atmosphere cell located between two N₂-filled ionization chambers used as detectors. The Cu-ZSM-5 and Cu-Al₂O₃ samples were calcined *in situ* in an oxygen flow at 773 K for 30 min, cooled to 523 K, and then contacted with a 2.4% NO, 1% C₃H₆, and 9.5% O₂ (balance helium) reaction mixture, with total flow 100 cm³·min⁻¹. After 30 min at 523 K, the sample was heated to 773 K at a constant rate of 0.35 K·min⁻¹. Gases 99.99% O₂, 5.5% NO in helium and 2.2% C₃H₆ diluted in helium (Scott Specialty Gases) were used as provided without further purification.

The energy scale was calibrated by simultaneously measuring a Cu foil (Johnson-Matthey, absorbance 1.5), located next to the reaction cell, using a third ionization chamber.

(D) Mathematical Description and Procedure. XANES spectra were energy-corrected by assigning an energy of 8979.0 eV to the first inflection point of the Cu foil spectrum, simultaneously measured with the sample, and subtraction of the pre-edge was performed with a linear combination of Victoreen and straight lines. Next, absorbance spectra were normalized to one for the post-edge atomic contribution at 9009.0 eV. This post-edge background was obtained by means of a cubic spline smoothing procedure²⁰ of the XAS spectrum up to 9300 eV.

The set of normalized spectra was submitted to a statistical analysis. For this purpose, a Fortran-code program was developed to perform Factor Analysis. FA²¹ can be applied when the variable under study, like absorbance in a set of XANES spectra, can be mathematically represented as a linear sum of uncorrelated components (called *factors*), provided that the number of spectra is larger than that of the components. An important property of this method lies in the fact that every factor makes a maximum contribution to the sum of the variances of the variable. Thus, it allows one to reduce a large body of data to a manageable (interpretable) set of basis functions (spectra).

The target of FA is to decompose a data matrix **D**, constituted of *c* spectra, into a *row matrix*, **R**, and a *column matrix*, **C**, so that:

$$\mathbf{D}_{r \times c} = \mathbf{R}_{r \times n} \cdot \mathbf{C}_{n \times c} \quad (1)$$

where subscripts indicate the dimensions of the matrices: *r* is the number of data points of a spectrum and *n* is the number of factors. The *row matrix* contains basic spectral components and the *column matrix* the concentration of the components in each original spectrum of **D**. The first part of FA, the Abstract Factor Analysis (AFA), consists of decomposing **D** into a product of two matrices:

$$\mathbf{D} = \mathbf{R}^\# \cdot \mathbf{C}^\# \quad (2)$$

This is done by diagonalizing the covariance matrix of **D** (that is, **Z** = **D**^t·**D**, where **D**^t is **D** transpose, and it is assumed *r* > *c*) using the Householder-QL algorithm.²² The algorithm generates an orthonormal matrix **Q**, containing the eigenvectors of the **Z** matrix, and a diagonal matrix, with the corresponding eigenvalues, both with dimensions *c* × *c*. From the diagonalization procedure it follows that:

$$\mathbf{C}^\# = \mathbf{Q}^t \quad (3)$$

where **Q**^t is **Q** transpose, and from eqs 2 and 3:

$$\mathbf{R}^\# = \mathbf{D} \cdot \mathbf{Q} \quad (4)$$

Through the analysis of eigenvalues, it is decided which are the *n* principal components and which ones correspond to experimental *noise*.

It should be stressed that *noise* has important contributions from background subtraction errors in the Cu K-edge.²³ Then, reduction of **R**[#] and **C**[#] matrices gives the *abstract* solution, so called because it is a mathematical solution to eq 1 without physical meaning.

Determination of the number of factors, *n*, is normally based on statistical tests^{21,24} and analysis of the abstract **R**[#] matrix.²⁵ To decide if any *k*th component (*k* = 1, ..., *c*) corresponds to signal or contains only *noise*, an *F* test²⁴ of the variance associated with the *k*th component and the summed variance associated with noise components (*k* + 1, ..., *c*) is performed. The percentage of significance level (% SL) gives the probability for the ratio *F* of both variances being higher than the calculated value. The *k*th factor is accepted as a principal component if % SL is lower than a test level. In previous results^{23,26} we found that this is one of the most reliable methods to determine the number of principal components, *n*. The test level was fixed to 5% based on the sharp increase observed in % SL value for the first noise component. To help in deciding the number of principal components, we used the reduced eigenvalue ratio (REVR) as well. The REVR, the ratio of two consecutive reduced eigenvalues, approaches one when two error eigenvalues are compared but it is significantly greater if one eigenvalue is responsible for signal.²¹

As will be shown later, for the present set of XANES spectra, neither REVR nor the *F* test unambiguously determine the number of pure species. For this reason, eigenvalues have been interpreted by means of evolving factor analysis, EFA,^{21,27} that allows one to introduce chemical information into the mathematical procedure. EFA is performed in an evolutionary process by repeatedly calculating eigenvalues while successively adding spectra to the **D** matrix as the evolutionary variable increases (forward EFA) or decreases (backward EFA). In this way, appearance of a new species is identified by an eigenvalue emerging from the pool of error eigenvalues. In this paper, the EFA procedure is interpreted in a new way. Unlike in chromatography,²⁸ the experimental technique in which the EFA method is widely used, we have no previous information on the order in which species appear or disappear as the evolutionary variable, the temperature in our case, changes. Thus, EFA diagrams are interpreted on the basis of temperature intervals at which different kinds of species exist. Such intervals are envisaged from a visual inspection of XANES spectra as Cu¹⁺ and Cu²⁺ oxidation states, corresponding to Cu ions inserted in oxo complexes or oxide matrixes or ZSM-5 exchanged ions, can be readily differentiated by their pre-edge XANES shapes.¹⁰ This fact gives us enough information to unambiguously choose the number of principal components and their regions of existence.

To interpret EFA diagrams, it is important to keep in mind the meaning of an eigenvalue, in order to understand the relationship between the development of chemical species and the evolution of eigenvalues. Eigenvalues represent the projections of the **D** matrix on a set of unit vectors (eigenvectors) that constitutes an orthogonal basis in a finite-dimensional space. The dimension of this space, that is, the number *n* of pure chemical species in our example, is expected to be lower than *c*, i.e. the number of columns of **D** (assumed to be lower than that of rows, *r*). However, because of the experimental error, besides the *n* eigenvectors corresponding to real components (factors), *c* - *n* non-zero error eigenvectors are obtained. Then, the *n* largest eigenvalues (primary eigenvalues) are associated with true species, including some error, and the *c* - *n* smallest eigenvalues (secondary eigenvalues) are composed of pure error.²¹

When performing forward EFA, we calculate eigenvalues for a **D** matrix containing the first two columns, then repeat after adding the 3rd column, etc., up to the point where *c* columns have been added, one at a time. For backward EFA, the process starts with the *c*th column and ends when adding the first one. From the interpretation of an eigenvalue given before, it follows that: (a) when adding a new column to the **D** matrix, if it contains a contribution from a species already present in previous columns, the corresponding eigenvalue increases (as the new column will have a contribution to the total projection on that eigenvector); (b) if one of the existing species is not in the new column, that is, the projection on a given basis vector is not altered by adding the new column, the corresponding eigenvalue remains constant; (c) if the added column shows a new species, a new eigenvalue emerges from the pool of noise eigenvalues.

After determination of the number of principal components by EFA, the final step in the FA procedure involves the rotation of the abstract **R** and **C** matrices to obtain the physically meaningful (real) solution. That is, a transformation matrix **T** is found so that:

$$\mathbf{C}_{\text{real}} = \mathbf{T} \cdot \mathbf{C}_{\text{abs}} \quad (5)$$

$$\mathbf{R}_{\text{real}} = \mathbf{R}_{\text{abs}} \cdot \mathbf{T}^{-1} \quad (6)$$

The **T** matrix is calculated by a self-consistent iterative process based on iterative transformation factor analysis (ITFA), also known as self-modeling curve resolution.²⁹ Concentration profiles and spectral components are self-consistently optimized until no physically meaningless features are observed. To determine the starting point in the iterative process, the **C** matrix is orthogonally transformed by a varimax rotation³⁰ to approach concentration profiles to curves showing maxima. Temperatures at which every pure component exhibits a maximum concentration are used to define uniqueness (TEST) vectors and subject to testing and refinement by iteration. A transformation matrix **T** is obtained as

$$\mathbf{T} = (\text{TEST}) \cdot \mathbf{C}_{\text{abs}}^t \quad (7)$$

and used to reproduce TEST vectors. New TEST vectors are refined by setting to zero any emerging negative value and then introduced in the iterative cycle. The convergence criterion is accomplished when the error in TEST vectors is lower than the real error.²⁹ The abstract row matrix is then rotated according to eq 6. Refinement of these spectral components leads to a new set of concentration profiles that are used as TEST vectors in the first iterative cycle. The whole process is repeated until convergence is reached.

Acknowledgment. The authors are indebted to Drs. W. K. Hall, M. Shelef, and K. C. Hass for a critical reading of the manuscript. We appreciate and thank Dr. K. C. Hass for providing us with a preprint of ref 12b. This work was supported under Project CAM-060/92 (Spain). C.M.A. acknowledges a short-period grant-in-aid from “Comunidad de Madrid”. M. F.-G. thanks the Spanish “Ministerio de Educación y Ciencia” for a postdoctoral fellowship. XANES spectra were obtained at CHESS, Cornell University, which is supported by the NSF. Financial support for the X-ray absorption work at CHESS was provided by the Office of Basic Energy Sciences, DOE.

Note Added in Proof. Recently Hwang et al.⁴³ have reported the critical influence of the copper phase distribution on the catalytic properties of Cu-ZSM-5 systems using DRIFTS. For an 80% exchanged Cu-ZSM-5 catalyst, at least two types of copper species are claimed to yield N₂ during the selective NO reduction using independent reaction paths. These results can be viewed as complementary of those reported by Adelman et al.³⁷ and discussed in the text. In any case, it may be stressed that although several copper species may exhibit activity in the SCR-HC reaction, our results show the catalytic predominance of the CuO-like phase when they co-exist.

JA961629Y

(43) Hwang, I. C.; Kim, D. H.; Woo, S. I. *Catal. Lett.* **1996**, *42*, 177.